COLLISIONALLY BORN FAMILY ABOUT 87 SYLVIA

2010 The Astronomical Journal 139 2148

(http://iopscience.iop.org/1538-3881/139/6/2148)

The Astronomical Journal, 139:2148–2158, 2010 June doi:10.1088/0004-6256/139/6/2148

COLLISIONALLY BORN FAMILY ABOUT 87 SYLVIA

David Vokrouhlický[1], David Nesvorný[2], William F. Bottke[2], and Alessandro Morbidelli[3]
[1] Institute of Astronomy, Charles University, V Holešovičkách 2, CZ-18000 Prague 8, Czech Republic; vokrouhl@cesnet.cz
[2] Southwest Research Institute, 1050 Walnut Street, Suite 300, Boulder, CO 80302, USA; davidn@boulder.swri.edu, bottke@boulder.swri.edu
[3] Observatoire de la Côte d'Azur, Dept. Cassiopee, 06304 Nice Cedex 4, France; morby@obs-nice.fr
Received 2009 November 20; accepted 2010 March 16; published 2010 April 14

ABSTRACT

There are currently more than 1000 multi-opposition objects known in the Cybele population, adjacent and exterior to the asteroid main belt, allowing a more detailed analysis than was previously possible. Searching for collisionally born clusters in this population, we find only one statistically robust case: a family of objects about (87) Sylvia. We use a numerical model to simulate the Sylvia family long-term evolution due to gravitational attraction from planets and thermal (Yarkovsky) effects and to explain its perturbed structure in the orbital element space. This allows us to conclude that the Sylvia family must be at least several hundreds of million years old, in agreement with evolutionary timescales of Sylvia's satellite system. We find it interesting that other large Cybele-zone asteroids with known satellites—(107) Camilla and (121) Hermione—do not have detectable families of collisional fragments about them (this is because we assume that binaries with large primary and small secondary components are necessarily impact generated). Our numerical simulations of synthetic clusters about these asteroids show they would suffer a substantial dynamical depletion by a combined effect of diffusion in numerous weak mean-motion resonances and Yarkovsky forces provided their age is close to ∼4 billion years. However, we also believe that a complete effacement of these two families requires an additional component, very likely due to resonance sweeping or other perturbing effects associated with the late Jupiter's inward migration. We thus propose that both Camilla and Hermione originally had their collisional families, as in the Sylvia case, but they lost them in an evolution that lasted a billion years. Their satellites are the only witnesses of these effaced families.

Key words: minor planets, asteroids: general

1. INTRODUCTION

The solar system has remained a crowded place for small bodies long after it emerged from its formation phase. In fact, mutual collisions continued to be an ubiquitous process until the present time (e.g., Nesvorný et al. 2006b; Nesvorný & Vokrouhlický 2006). Traces of collisional or tidal fragmentation events are seen in virtually all observed populations of small bodies, from Hungarias (e.g., Warner et al. 2009; Milani et al. 2010), the asteroid main belt (e.g., Zappalà et al. 2002; Cellino et al. 2002; Nesvorný et al. 2006a), resonant populations such as Hildas (e.g., Brož & Vokrouhlický 2008) or Trojans (e.g., Milani 1993; Beaugé & Roig 2001; Roig et al. 2008), to the trans-Neptunian region (e.g., Brown et al. 2007; Levison et al. 2008). Circumplanetary-wise, we have evidence for clusters of collisionally born irregular satellites (e.g., Nesvorný et al. 2004) and Saturn's rings are likely offspring from a past giant fragmentation (e.g., Charnoz et al. 2009). In each of these cases, analysis of the families of fragments provides a wealth of information of the dynamical circumstance of the collision, material strength, and fragmentation process of the parent object and its internal composition.

In this paper, we analyze collisionally born family about the large Cybele-zone asteroid (87) Sylvia. So far this region exterior to the main asteroid belt did not receive much attention, perhaps because only a limited number of objects has been known to populate it. Recent years though have seen a significant increase of newly discovered Cybele objects explained most readily by intrinsic properties of the size distribution function in this population (Section 2). This allows a more detailed scrutiny of objects in this heliocentric zone. Our search indicates that there is no detectable asteroid family in the Cybele zone other than that around (87) Sylvia. In particular, no statistically significant clustering of objects is seen about the other large asteroids including (65) Cybele, (76) Freia, (107) Camilla, (121) Hermione, and (168) Sybilla. The most notable cases of family absence are Camilla and Hermione which both have small satellites (such as Sylvia; e.g., Marchis et al. 2005a, 2005b, 2006, 2008a, 2008b; Descamps et al. 2009).

We point out this later aspect because of the predominant belief that Sylvia-class binaries or multiple systems interior to Jupiter's orbit, characterized by a large ($D \geqslant 100$ km) primary and a small ($D \leqslant 20$ km) secondary component, must have been born during a family forming event (e.g., Durda et al. 2004; Pravec & Harris 2007). Indeed, while the recent ideas about radiative-torque-driven pathways to rotational fission of small asteroids opened new possibilities for formation scenarios of small main-belt binaries, none of them is applicable to large systems. Thus assuming the large binary and multiple systems are collisionally born, we also would expect that they reside in recognizable asteroid families. The case of the Sylvia family, studied below, is a nice example. Yet, out of eight other known large binary systems, mostly in the outer part of the asteroid belt, only (283) Emma has an associated asteroid family and all others do not possess families (e.g., Nesvorný et al. 2006a; Marchis et al. 2008b). Such a disparity requires an explanation and potentially could lead us to interesting insights about processes in the early solar system. In this paper, devoted to the Cybele zone, we pay close attention to the case of two large, and family free, binaries: (107) Camilla and (121) Hermione. In particular, postulating existence of their past families, we try to understand how and on which timescale they could have been obliterated.

Basic information about the Cybele zone, relevant for our work, is summarized in Section 2. Our simulations, analysis, and interpretation are presented in Section 3. Conclusions

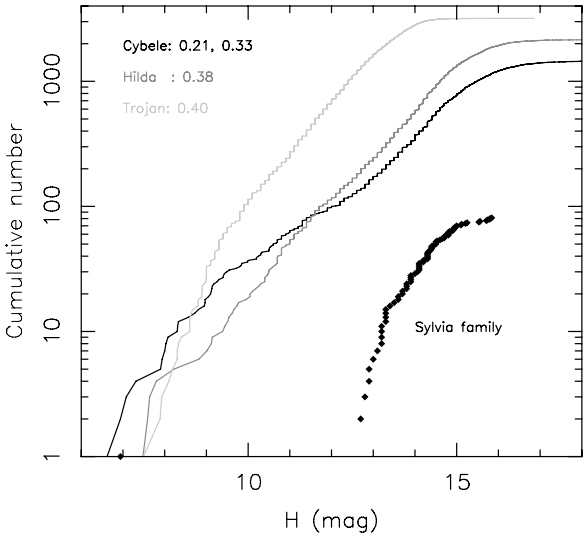

Figure 1. Cumulative absolute magnitude distribution $N(< H)$ for Cybele population (black), Hildas (medium gray), and Trojans (light gray). Using a piecewise "power-law" approximation $N(< H) \sim 10^{\gamma H}$, we obtain the following values of the exponent γ: (1) $\gamma \simeq 0.21$ in the H-interval (9.5, 12.5) and $\gamma \simeq 0.33$ in the H-interval (12.5, 15) for Cybele population, (2) $\gamma \simeq 0.38$ in the H-interval (12, 15) for Hilda population, and (3) $\gamma \simeq 0.40$ in the H-interval (9.5, 13) for Trojan population. Diamonds show cumulative distribution of Sylvia family members, significantly steeper that any of the other populations and characteristic to a collisionally born cluster of asteroids.

in Section 4 summarize our results as well as a couple of outstanding problems left for the future work.

2. WHAT DO WE KNOW FROM OBSERVATIONS?

Our initial search for Cybele-zone asteroids in available catalogs detected about 1500 objects as of 2009 June.[4] Of these bodies about 1000 were observed during more than one opposition, such that their orbits were reliable enough for further analysis. In what follows we thus used only the multi-opposition objects.

We first analyze the absolute magnitude H distribution of Cybele objects and put it in relation to the corresponding distribution functions of the neighbor populations: Hildas, Trojans, and outer main-belt asteroids. Figure 1 shows the cumulative $N(<H)$ distribution for three of these populations, including Cybele (black curve). Formation circumstances, long-term evolution, and internal physical properties are reflected in the typical wavy pattern of these distributions, but we note they can be piecewise approximated with a power law $N(<H) \sim 10^{\gamma H}$ and some slope exponent γ. These exponents are of interest for both comparison of neighbor populations and also for judging if the population is near to collisional steady-state situation (e.g., O'Brien & Greenberg 2003, and references therein).[5] We note that the magnitude distribution of the Cybele population is among the shallowest known in the solar system (this feature has been recognized already by Milani & Nobili 1985): γ value proceeds from ~0.21 to a slightly steeper value ~0.33 as one moves through the magnitude interval 9.5–14.5.[6] Such shallow values are not seen in Hildas, $\gamma \sim 0.38$ for H in between 12 and 14.5, and Trojans, $\gamma \sim 0.4$ for H in between 9.5 and 13 (Figure 1; Marzari et al. 2002). More importantly, they are also shallower than the corresponding power-law approximations of the outer main-belt population of asteroids, where we have $\gamma \sim 0.35$ for H in between 9 and 12 and $\gamma \sim 0.47$ for H in between 12.5 and 15 (e.g., Marzari et al. 2002). This latter comparison is of interest because the outer main-belt objects, which outnumber Cybeles by at least 2 orders of magnitude, are the prime projectiles driving Cybeles' collisional evolution. The collisional evolution of the Cybele zone over the past Gyr has yet to be understood in light of such a difference between the observed size/magnitude distributions. However, the comparison with other nearby populations allows us to hypothesize that the Cybele zone is perhaps the least collisionally processed population (for that reason, Milani & Nobili 1985 even proposed no sizable collisional families would be found in this region).

The overall paucity of objects beyond J2/1 mean-motion resonance with Jupiter, where some put the upper limit of the main asteroid belt, preoccupied dynamists since the 1970s. The work of Milani & Nobili (1985) summarizes some of the early work and presents a first significant effort to understand the small population of Cybele objects as a result of long-term orbital instability due to planetary gravitational perturbations. In particular, this work explains well why objects are nearly entirely missing beyond the J7/4 resonance (located at about 3.6 AU heliocentric distance) but fails to predict instability in between J2/1 and J7/4 resonances. Similarly, longer numerical integrations of Lecar et al. (1992) indicated the Cybele zone below[7] J7/4 resonance is overall stable (except discrete locations of weaker mean-motion resonances; see also results in Robutel & Laskar 2001). Our own integrations outlined below confirm this conclusion up to a previously unreached timescale of a billion years.

The problem became clarified by the work of Liou & Malhotra (1997) and Minton & Malhotra (2009). These authors showed that the heliocentric zone next to the outer parts of the asteroid main belt were efficiently depleted by sweeping mean-motion resonances when Jupiter and Saturn migrated into their final positions. According to what is known as the Nice model (Tsiganis et al. 2005; Gomes et al. 2005), this happened ~3.8–3.9 Gyr ago, shortly after terrestrial planets and the Moon were bombarded by projectiles from a destabilized outer planetary disk and numerous asteroids from the main belt zone. Levison et al. (2009, their Figure 1) have shown that some, but not many, of these projectiles also might have been captured in the Cybele zone. Since then, however, the stability of orbits in the Cybele zone was restored as proved by the previously mentioned works. Only regions immediately adjacent to planetary resonances might have been eroded by very slow, chaotic diffusion processes.

Another piece of information comes from spectroscopic and broadband photometric studies. Because of the distance to the Cybele targets, such data are not as numerous and detailed as for the near-Earth or inner main-belt asteroids. Yet the available

[4] Technically, the Cybele population objects have orbits in between the J2/1 and J3/2 (Hilda) mean-motion resonances with Jupiter. No significant mistake is performed when a simpler criterion for osculating semimajor axis a is used: $a > 3.33$ AU and $a < 3.8$ AU. In any case, the border-zone objects are not of importance for our work.

[5] Apparent magnitude of asteroids in the Cybele zone at opposition are about 1 mag fainter than their estimated absolute magnitudes H. As a result, we find it likely that their population might be complete at $H \sim 14$.

[6] This slightly steeper behavior of the magnitude distribution beyond $H \sim 12.5$ is responsible to the new discoveries in the past years; indeed, most of the $H > 13$ mag objects in the Cybele population were first observed during the past decade.

[7] In this paper, we adopt the usual terminology indicating objects with semimajor axis values smaller than the resonance being "below" the resonance and vice versa.

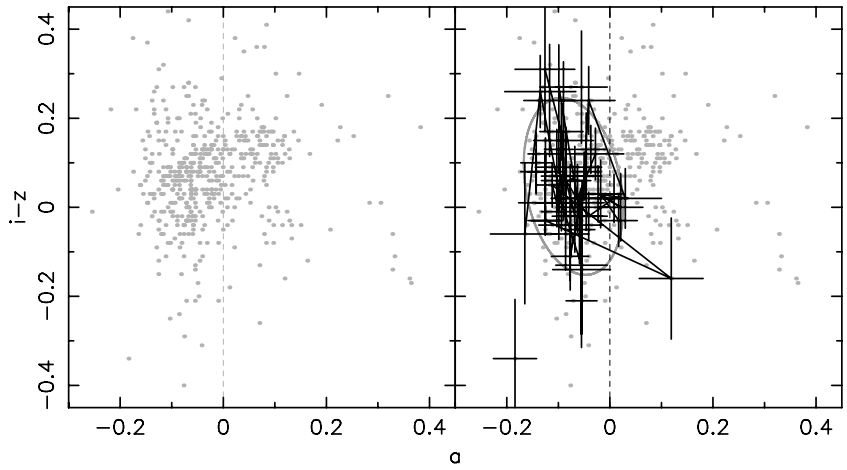

Figure 2. Color–color diagram based on reliable SDSS observations of the Cybele population (a^* is a linear combination of the fluxes in g, r, and i filters as stated in the text and in Parker et al. 2008). Left panel: all available observations of asteroids in the Cybele zone shown as gray dots. Right panel: dark crosses are observations of the Sylvia family members (with error bars). Lines connect multiple SDSS observations of a single object in the Sylvia family. The gray ellipse in the right panel indicates 90% confidence level zone of the Sylvia-family colors as determined from the observed members; its center is at $\overline{a^*} \sim -0.07$ and $\overline{i-z} \sim 0.05$. The dashed line at $a^* = 0$ divides flat spectra (to the left) and steep spectra (to the right).

spectral evidence also points toward a slight difference between the resonant populations in the outer belt (Hildas and Trojans) and Cybeles: the latter show a higher percentage of flat spectral types as compared to steeper spectra present among the former groups. This is most straightforwardly seen among the larger members. Out of 11 Cybele spectra in the SMASS II survey 10 are classified as C or Xc (e.g., Bus & Binzel 2002). Similarly, out of 31 Cybele spectra in the S2OS3 survey, some 2/3 are compatible with C and X classification and only six spectra of smaller objects were classified D (e.g., Lazzaro et al. 2004). Earlier, some authors proposed a generic trend from flat to steep spectra as one moves from large to small members in the Cybele population (e.g., Lagerkvist et al. 2005), but the most recent studies indicate such a size versus spectral-slope correlation does not actually exist (e.g., Karlsson et al. 2009; Gil-Hutton & Licandro 2010). Rather, there is a broader spread of spectral slopes as one moves toward small members in the Cybele population. Still, the flat spectra seem to dominate the population even at small sizes and this makes the Cybele population unlike Hildas (with about equal mixing of flat and steep spectra is observed; e.g., Brož & Vokrouhlický 2008) and Trojans (where the steeper spectra dominate among small members; e.g., Szabó et al. 2007; Roig et al. 2008).

To test this conclusion, we used Sloan Digital Sky Survey (SDSS; e.g., Ivezić et al. 2001; Parker et al. 2008) data and extracted reliable observations of Cybele members (see also an independent analysis in Gil-Hutton & Licandro 2010). Using methodology in Parker et al. (2008) we constructed color indexes $a^* = 0.89\,(g-r) + 0.45\,(r-i) - 0.57$ and $i-z$, based on the SDSS 4 filter observations (leaving aside the often noisy u filter), and eliminated data that had too large formal errors in both colors. We thus obtained 485 observations for 241 different Cybele objects (a significant fraction of the overall observed Cybele population; Figure 2). Note that one object may be observed several times during the SDSS program. Comparisons of different observations of a single target may show differences that have been analyzed by Szabó et al. (2004). Based on their work we prefer to include all observations in our analysis, rather than computing mean colors for a given target. The average absolute magnitude of the SDSS-observed targets among Cybele population was ∼13.8, so these data provide information about spectra of smaller end objects in the population. Out of the 485 individual observations, some 333 have a^* index smaller than 0 which indicates flatter spectra (e.g., Parker et al. 2008, their Figure 3). Hence some 2/3 of all SDSS observations of Cybele small objects indicate their connection to the C/X spectral complex.

2.1. Sylvia Family

Nesvorný et al. (2006a) were the first to notice a cluster of Cybele objects around the large asteroid (87) Sylvia. At that time, however, the number of known members in this family was small and prevented any detailed study. In this paper, we make use of a fast increase of discoveries of small objects across all populations in the solar system during the past few years. We show that the current population of known Cybele objects allows us a more detailed study of this family.

In the first step, we searched for asteroid families about large members in the Cybele population. To that end, we used two different sources of orbital data that yielded the same results and allowed thus the same conclusions. First, we used the catalog of synthetic proper orbital elements provided by AstDyS Web site (e.g., Knežević et al. 2002). These are currently computed for numbered objects only and we thus identified 640 numbered Cybele objects in this source as of 2009 July. Performing search for statistically significant clusters of objects about the 10 largest Cybele asteroids, we noted that only (87) Sylvia has a clear family in this population. Using the classical hierarchical clustering approach (HCM) of Zappalà et al. (1990), we identified 56 Sylvia family members at the cutoff velocity of 110 m s^{-1} (comparable to its escape velocity). The only other case of a possible clustering is around (909) Ulla with about six to eight neighbor members at the 100 m s^{-1} cutoff velocity. This cluster is, however, still insignificant and more objects discovered in its surrounding are needed to confirm, or disprove, this other cluster. We specifically note that no clusters are found around asteroids (107) Camilla and (121) Hermione.

In the second approach, we integrated all 1013 multi-opposition objects as of 2009 July in the Cybele zone (numbered and non-numbered) over 2 Myr and determined their mean orbital elements: semimajor axis, eccentricity, and

inclination. Such time averages are not the synthetic proper elements of Milani and Knežević, because they also contain the forced planetary contributions in eccentricity and inclination. However, the range of heliocentric distances in the Cybele zone is small enough that these average orbital elements are still suitable proxies of the proper elements and can be used for our analysis.[8] They are especially useful in the long-term integrations described in Section 3, where a full implementation of the synthetic proper elements over a running interval of time would be too computationally expensive. We performed the same HCM analysis using the averaged orbital elements of Cybele asteroids and again found only one statistically significant cluster: the Sylvia family. At 110 m s^{-1} velocity cutoff it now contains 81 members (including Sylvia). This larger number of family members, compared to 56 above, does not have to do with differences in the definition of orbital elements but is due to the larger database: the synthetic elements are available for the numbered asteroids only while we computed our averaged elements for all multi-opposition objects. In particular, all 56 numbered asteroids in the Sylvia family are found in both its realizations, while that constructed from the time-averaged orbital elements contains additionally 25 multi-opposition, but non-numbered objects.

We now summarize basic facts about the Sylvia family. Figure 1 shows absolute magnitude distribution of its members as defined from our second approach, i.e., using 81 numbered and non-numbered asteroids. We note a huge gap between (87) Sylvia and other members in the family which indicates the family results from a large cratering event. Considering the observed members only, we would estimate the mass ratio of Sylvia and the parent object of its family be ∼0.99. This is obviously an overestimate because the number of small members in this family were not discovered yet and their size distribution is very steep. To reliably determine this mass parameter, one would need to use techniques similar to those in Durda et al. (2007) who compared results from the numerical modeling of fragmentation process to the observed size distribution of the largest fragments. This way they were able to account for the unseen mass in small fragments and determine the mass ratio of the largest fragment to the parent body in a more reliable way. However, because of the C/X type classification of (87) Sylvia, and its family members, strictly speaking we are not allowed to use results in Durda et al. (2007) who adopted a solid rock material properties for the projectiles and targets in their work. It though seems plausible that the discussed mass ratio between the largest fragment and parent body in this family will be >0.9.

The fact that we are dealing with a large cratering event on Sylvia itself also helps us to understand the process of the family identification in a little more depth. We recall that the standard HCM technique (see, e.g., Zappalà et al. 1990) constructs a chain of objects whose mutual velocity distance is smaller than a chosen cutoff, 110 m s^{-1} in our case. However, this implementation does not take into account masses of the bodies and seeks to link them in a democratic way as if masses of all members were comparable. The case of Sylvia is different and it is actually more relevant to express velocity differences with respect to Sylvia itself. Still, the most distant family members, near the J9/5 mean-motion resonance, have the relative velocity with respect to Sylvia of ∼110 m s^{-1}, well compatible with the estimated escape velocity. Because (87) Sylvia, residing at $\bar{a} \sim 3.485$ AU, is miscentered toward smaller semimajor axis value with respect to an average computed over other members of our nominal family (Figures 3 and 4), we might consider a possibility that some fragments might have also been launched below the J11/6 resonance. Indeed, the minimum necessary relative velocity with respect to (87) Sylvia is ∼60 m s^{-1} for those orbits, but no fragments associated with our nominal HCM-defined family at even 110 m s^{-1} because population of objects below J11/6 resonance is much more scattered in the proper element space. On the other hand, to get the Sylvia family initially extent beyond the J9/5 mean-motion resonance, see the top and left panels in Figures 3 and 4 where some asteroids reside on comparable eccentricity and inclination values, we would need relative velocities with respect to (87) Sylvia exceeding 110 m s^{-1}. This is not impossible and some of these objects residing between 3.53 and 3.56 AU could be Sylvia members. To stay conservative, though, we decided to consider the Sylvia family identified at 110 m s^{-1} HCM cutoff a minimum and reliable guess; this nominal family thus extends in between J11/6 and J9/5 mean-motion resonances. Increasing the HCM cutoff would merely imply some objects beyond J9/5 would start to be associated with the family, but this does not change any fundamental conclusions from our work.

With that said the structure of the nominal family in proper/averaged orbital element space still presents some interesting puzzles. The most notable of them is the larger eccentricity and inclination dispersion of the Sylvia members for $a > 3.492$ AU (Figures 3 and 4). Another interesting feature is a non-uniform distribution of the Sylvia members in semimajor axis which has three maxima: (1) two adhering to the resonances J11/6 and J9/5 (the most significant one) and (2) the last in the region in the immediate zone of the asteroid (87) Sylvia. The first two indicate there was a kind of piling up of the Sylvia members toward the resonances, most easily explained by the Yarkovsky forces (see, e.g., Vokrouhlický et al. 2006a, 2006b, and Section 3.1 here).

We now give a look at what SDSS observations may hint about the nature of the Sylvia family. The fact that (87) Sylvia itself is classified C or Xc would imply the family must be of this classification. Indeed, SDSS provides 51 individual color indexes of 21 different objects in the Sylvia family (Figure 2) and 48 of them have $a^* < 0$. This classifies them into the C/X complex. Using these 51 observations of the a^* and $i-z$ indexes for the Sylvia family members, we constructed a two-dimensional 90% confidence level that defines the family (see the gray ellipse in Figure 2; we used the technique described in Bertotti et al. 2003, Section 20.5). Again, the mean values of a^* and $i-z$ characterize the family to be of flat, C/X-type compatible spectra.

Finally, we recall that (87) Sylvia has two resolved small satellites (e.g., Marchis et al. 2005a, 2006) whose sizes are typical for other members in the Sylvia family. It is very likely that these satellites were formed at the same time, and by the same process, as the Sylvia family (e.g., Durda et al. 2004). In this respect, we find it a priori puzzling that the other two large Cybele asteroids that have small satellites—(107) Camilla and

[8] The time-averaged orbital elements are very close to the free (proper) elements when the amplitude of the forced terms is small. This is very well satisfied for inclination values. The proper inclination for Sylvia members is ∼9.°7, while the most significant forced term of s_6 frequency has an amplitude of ∼0.°5–0.°6 only. In the case of eccentricity, the proper values in the Sylvia family range between ∼0.053 and ∼0.065, while the largest forced terms are associated with g_5 and g_6 frequencies and have amplitudes of ∼0.037 and ∼0.016. Because our averaging window is significantly longer than the periods of the proper and forced cycles, and there is no resonance between them, the average values of eccentricity are just shifted by a constant value ∼0.011–0.012 with respect to the proper terms. This difference cannot affect any conclusions from our work.

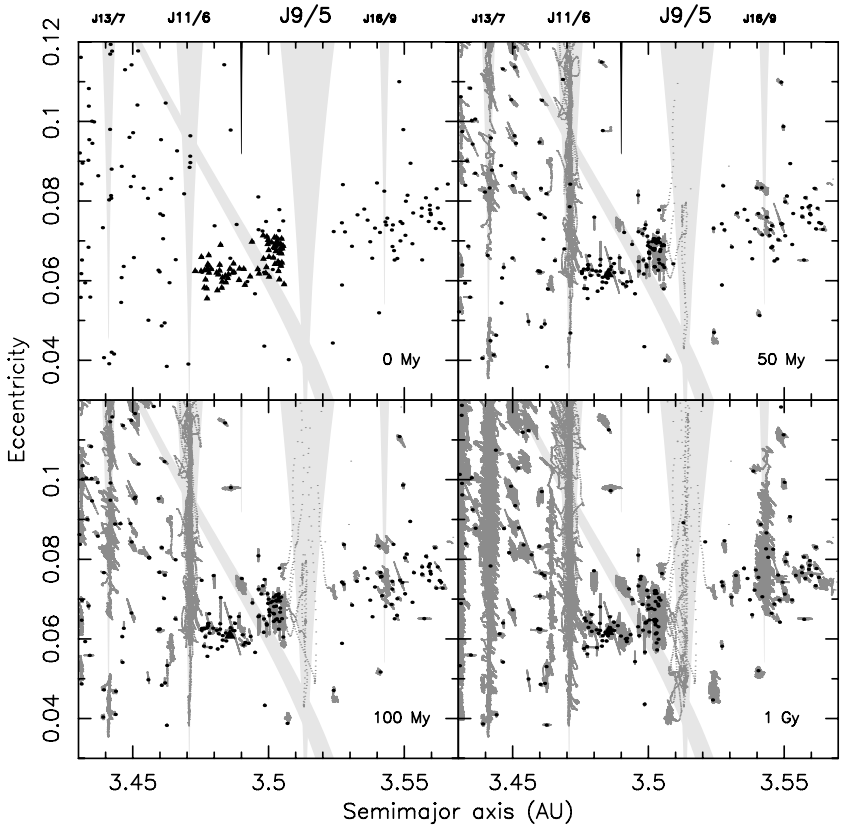

Figure 3. Snapshots of the orbital evolution of Cybele asteroids in the zone near Sylvia family. The axes are mean semimajor axis and mean eccentricity values averaged over a 2 Myr running window. The left upper panel shows the values obtained during the first 2 Myr of our integration ("current values"); the cluster shown by triangles indicates the Sylvia family at 110 m s^{-1} HCM cutoff. Note that (87) Sylvia with mean semimajor axis ∼3.485 AU and mean eccentricity ∼0.062 resides near the center of the bottom clump of triangles at smaller heliocentric distances; henceforth, its position is significantly displaced from the center of the whole family. The other panels show situation after 50 Myr elapsed (right and top), 100 Myr elapsed (left and bottom), and 1 Gyr elapsed (right and bottom); position of (87) Sylvia is shown by a triangle. The gray dots show evolutionary tracks of the integrated objects and the black dots are mean elements during the last 2 Myr of integration in that panel. Light gray vertical zones delimit positions of the mean-motion resonances with Jupiter; the most notable cases are J9/5, J11/6, J13/7, and J16/9 slowly depleting the zone near 3.54 AU semimajor axis value. The transversal light gray zone indicates position of the z_1 secular resonance for the mean value of the inclination in the Sylvia family (∼9.°5).

(121) Hermione—do not posses families of fragments around them (see Section 1). This issue is being discussed in a more detail in the following section.

3. WHAT DO WE CONCLUDE FROM MODELING?

In this section, we use a numerical model to analyze some of the puzzling facts we described in the previous section. We first focus on the structure of the Sylvia family. We note that the zone below J11/6, accessible to a high-velocity tail of fragments launched during the original breakup of the parent body of the Sylvia family, becomes unstable due to planetary perturbations on a several hundred Myr timescale. Henceforth, it is quite possible that some Sylvia members have been initially launched into this orbital zone but did not survive until the present time. Next, we pay a closer look at the unequal structure of the family below and above the proper semimajor axis value of ∼3.492 AU. Observing this structure is reminiscent of that in the Koronis family (e.g., Bottke et al. 2001), we postulate it has been produced by a steady flow of Sylvia members across a weak secular resonance located at this heliocentric distance and interaction with weak mean-motion resonances adjacent to J9/5. Indeed, we find that the Sylvia family is crossed with a prominent secular resonance $z_1 = g + s - g_6 - s_6 = \nu_6 + \nu_{16}$ (e.g., Milani & Knežević 1992, 1994); the same also is responsible for the perturbed structure of Eos and Agnia families in the inner and outer parts of the asteroid main belt (e.g., Vokrouhlický et al. 2006b, 2006c). Numerical simulations that include the Yarkovsky forces (e.g., Bottke et al. 2002, 2006) confirm that an outward flux of the Sylvia members through this resonance allowed us to acquire the observed higher eccentricity and inclination orbital dispersion (Section 3.1). Because this process is time dependent, it provides us with yet another constraint on the lower bound of the Sylvia family age consistent with the necessary depletion timescale of the zone below the J11/6 resonance.

We next turn to the topic of currently missing families about (107) Camilla and (121) Hermione (Section 3.2). Our perspective follows a canonical view that their satellites were born during the family forming breakup or cratering event of Camilla and Hermione predecessors. Obviously, a possibility is that the corresponding cratering event created a family of fragments below our current resolution. However, this solution to the problem does not seem likely given the satellite sizes >15 km (e.g., Pravec & Harris 2007; Marchis et al. 2008a; Descamps et al. 2009). Leaving aside the possibility that Camilla's and Hermione's satellites were created by some yet unknown mechanism for the moment, we are directed back to the question: why do these two large asteroids not have their families? Using a numerical model, we argue that these families did exist in the past but they dispersed during the Gyr-long orbital evolution due to (1) a combination of thermal and

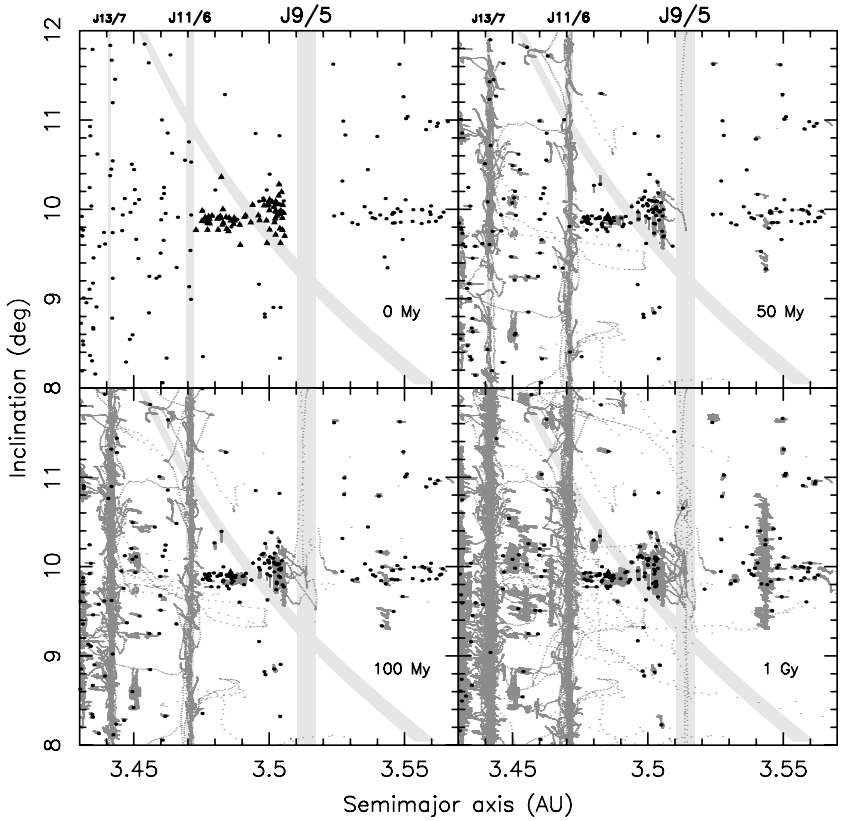

Figure 4. Same as in Figure 3 but now the axes are mean semimajor axis and mean inclination averaged over a 2 Myr running window. The z_1 resonance is shown for the mean value of the eccentricity in the Sylvia family (∼0.06).

gravitational perturbations during the past ∼3.8 Gyr and (2) an initial perturbation due to the effect of resonance sweeping through this orbital zone before ∼3.8 Gyr (not modeled in this paper). All these lines of evidence push the age of the putative Camilla and Hermione families to be larger than ∼3.8 Gyr. Today, no traces of these past families have remained other than the two satellites.

Our numerical integrations were performed using the symplectic scheme known as SWIFT_RMVS3 (see Levison & Duncan 1994). In some simulations, we included effects of the thermal (Yarkovsky) forces. For this task, we used their implementation in SWIFT described by Brož (2006). We used perturbations by all planets with their ephemerides at MJD55000.0 taken from the JPL DE405 file. The asteroid orbital data were taken from the AstOrb database as of 2009 June. The integration timestep was 5 days and most of the simulations were ended at 1 Gyr (unless all particles escaped or were otherwise terminated before) with some of them pushed to 2 Gyr. To prevent disk overflow, we output state vectors of planets and asteroids once every 2 kyr. This is not enough dense for a detailed study of residence in mean-motion resonances, but quite sufficient for our main purposes. For instance, it allows us to compute evolution of the mean orbital elements—semimajor axis, eccentricity, and inclination—over a 2 Myr wide running window.

3.1. Sylvia-family Zone Analysis

First we address the topic of orbital stability in the immediate zone of the Sylvia family. To that goal, we restricted our list of multi-opposition asteroids in the Cybele zone to those having osculating orbital elements in the following region: (1) semimajor axis in the 3.35–3.57 AU interval, (2) eccentricity less than 0.15, and (3) inclination in the 7°–13° interval (to verify we did not miss any important objects we also ran shorter—100 Myr—integration of asteroids in an extended zone with eccentricities up to 0.2 and inclinations in between 5° and 15°). We integrated orbital evolution of the selected 425 objects, obviously including the 81 multi-opposition identified members of the Sylvia family, for 1 Gyr including gravitational perturbations by all planets. Since we are mainly interested in the underlying chaoticity of the orbital zone surrounding the Sylvia family, we did not include effects of the thermal forces in this initial simulation.

Snapshots of the orbital evolution from this simulation at 0, 50 Myr, 100 Myr, and 1 Gyr are shown in Figures 3 (semimajor axis versus eccentricity projection) and 4 (semimajor axis versus inclination projection). The black triangles in the upper and left panels show Sylvia-family members as identified from the current orbital elements. The gray dots in the remaining panels show evolutionary tracks computed as averaged elements over a 2 Myr running window with an incremental step of 50 kyr. The black points are the last-computed averaged elements for that epoch. Many orbits, especially those above the J11/6 mean-motion resonance with Jupiter are fairly stable such that their evolutionary tracks (in gray) are not even seen and coincide with the black points. We note that the basic structure of the Sylvia family at 1 Gyr is basically the same as at the beginning of our simulation. We point out that even the zone beyond the J9/5 resonance is fairly stable except for the zone of the J16/9 mean-motion resonance with Jupiter at ∼3.54 AU. On the other hand, a number of orbits below the J11/6 resonance, and obviously those which happened to reside in or very near one of the major mean-motion resonances with Jupiter, exhibit instability and were eventually eliminated from our simulation. The corresponding dynamical timescales ranged from tens to

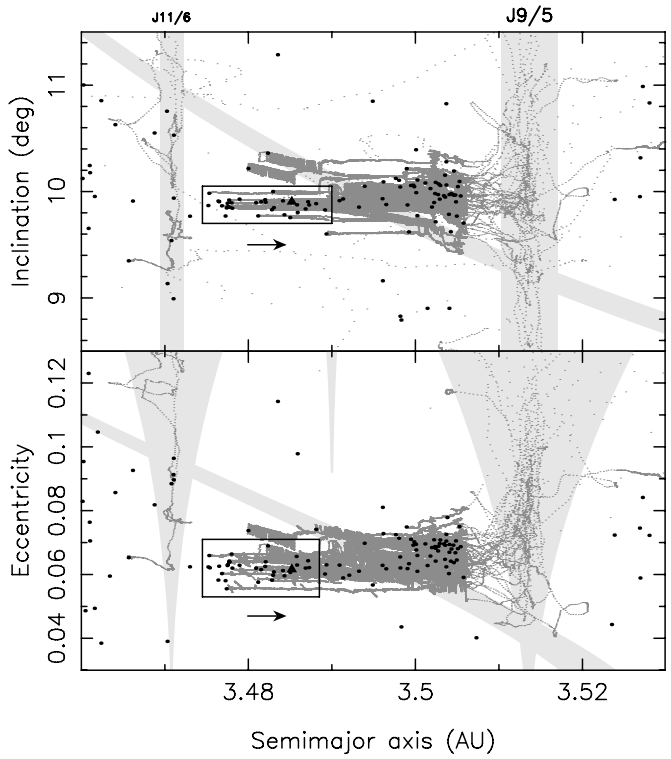

Figure 5. Evolutionary tracks (gray) of 40 asteroids started mostly in the core of the Sylvia family near the largest member (87) Sylvia (square zone). The axes are averaged orbital elements over a 2 Myr running window: semimajor axis vs. inclination (top) and semimajor axis vs. eccentricity (bottom). Gravitational perturbations from all planets and maximum Yarkovsky force for $D \sim 5$ km objects used in the simulation that cover about 0.5 Gyr of evolution (the arrow indicates direction by which the thermal forces make the orbits migrate). Black symbols are asteroids in the Sylvia family and some in its surrounding zone (top left panels in Figures 3 and 4); position of (87) Sylvia is shown by a triangle. Upon crossing the z_1 secular resonance, diagonal gray strip, the dispersion of the mean orbital eccentricity and inclination values increases. Eventually, the outward migrating objects are removed by the J9/5 mean-motion resonance with Jupiter at $a \simeq 3.515$ AU (all except a single body in our simulation).

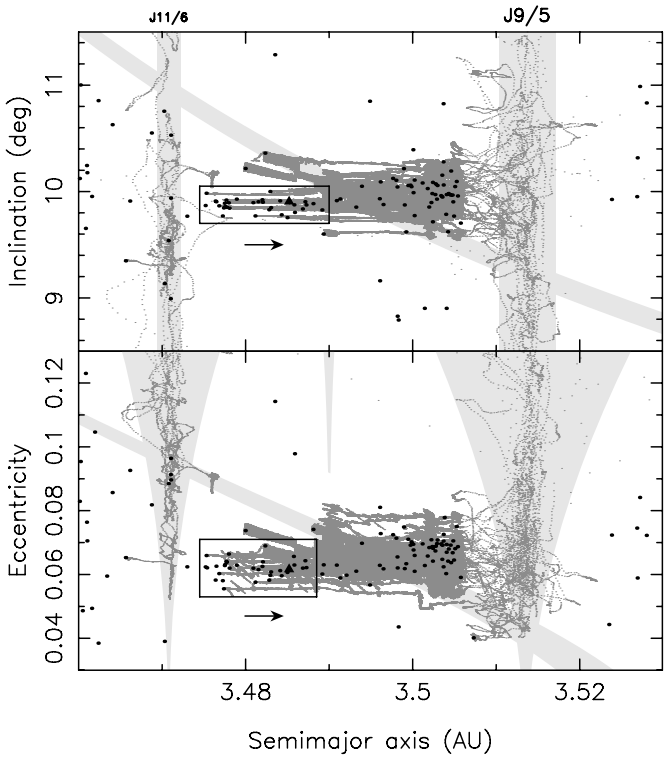

Figure 6. Same as in Figure 5 but now the mean semimajor axis drift da/dt corresponds to a maximum value estimated for the $D \sim 15$ km objects (i.e., three times slower than in the previous figure). In this case, no objects crossed the J9/5 mean-motion resonance with Jupiter.

hundreds of Myr. The fact that some ~10 km size asteroids initially residing in the Sylvia family were eliminated from our simulations through the resonances on a timescale shorter than the age of the family also resembles the previously studied situation in the Koronis family (see Milani & Farinella 1995; Vokrouhlický et al. 2001 for details).

Results from our integrations have the following implications. Comparing the Sylvia family members in between J11/6 and J9/5 at 0 and 1 Gyr epochs, we do not see a significant difference. Hence the core zone of the family is fairly stable and may dynamically survive 1 Gyr (and possibly even 4 Gyr). The zone below J11/6 is unstable on a timescale of several hundreds of Myr. Out of 48 objects initially in the zone between J13/7 and J11/6 resonances, only 25 survived 1 Gyr of orbital evolution and some were pushed to the resonance zones at the end of our simulation (awaiting thus further elimination) or were displaced from their initial positions. If the Sylvia family age is at least that long, some initial fragments that might have been ejected into this zone were likely dynamically eliminated. The current population of asteroids in between J13/7 and J11/6 (top and left panels in Figures 3 and 4) could be in part residual of the Sylvia members and also some background asteroids pushed to their location by thermal forces.

Next we analyze a possible source of eccentricity and inclination scatter beyond ~3.492 AU heliocentric limit in the Sylvia family. Our working hypothesis is that this feature have been produced by an outward flow of objects through the z_1 secular resonance shown by the diagonal gray interval in Figures 3 and 4 (indeed, the onset of the scatter exactly coincides with the location of this resonance as seen in these figures). To test our idea we performed two numerical simulations with a limited number of asteroids, 40 in each case. The initial conditions for both simulations were identical and were those of several Sylvia-family asteroids located near the asteroid (87) Sylvia at $a \sim 3.475$–3.485 AU. We included both the gravitational perturbations due to all planets and the Yarkovsky forces in our simulation. The latter were chosen such that they produced maximum estimated secular drift of the semimajor axis for a 5 km size member of the Sylvia family (the first simulation) and 15 km size member of the Sylvia family (the second simulation).[9] Figures 5 and 6 show results of our simulations. Indeed, we see that upon reaching the z_1 resonance, and a network of weak mean-motion resonances with Jupiter adjacent to J9/5, the eccentricity and inclination dispersion of the propagated orbits increases by about 50%. This is comparable to what we currently see in the family (black symbols show mean orbital elements in the surrounding zone of the Sylvia family, including the family itself). The evolution from the source zone near the center of the family to the zone adjacent to the J9/5 resonance took on average ~250 Myr for 5 km size asteroids and about three times longer for the 15 km size

[9] This size range roughly brackets that of the observed members in the Sylvia family (except for 87 Sylvia). We used a diurnal variant of the Yarkovsky effect only and estimated density for (87) Sylvia of ~1.2 g cm^{-3} (e.g., Marchis et al. 2008a). This provides $da/dt \sim 5 \times 10^{-5}$ AU Myr^{-1} for the 5 km size bodies and three times smaller value for the 15 km size bodies (e.g., Bottke et al. 2002, 2006).

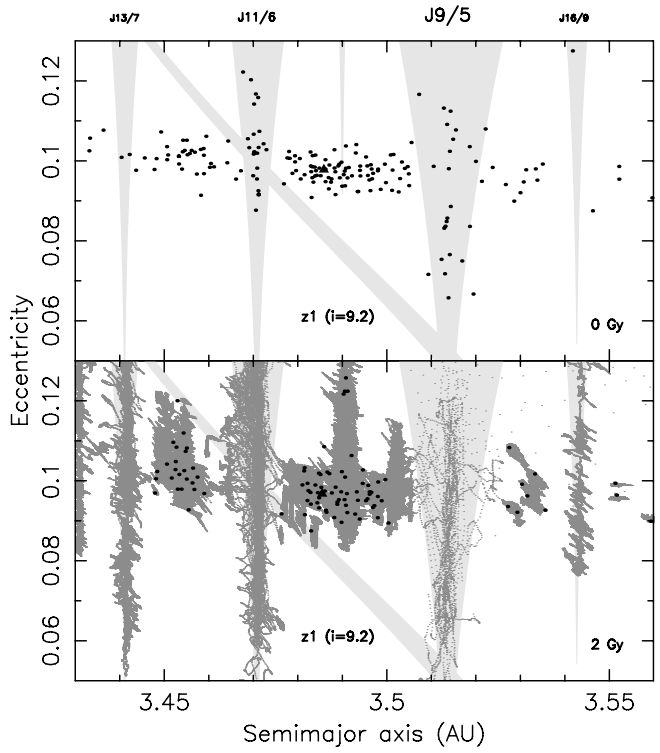

Figure 7. Orbital evolution of a simulated synthetic family about (107) Camilla (black triangle); averaged orbital elements over a 2 Myr running window used on the axes. Top panel shows the first 2 Myr of integration (i.e., the initial simulated family), bottom panel shows situation after 2 Gyr of evolution. The gray dots are evolutionary tracks of the mean elements and black points are those in the last 2 Myr of the simulation. Gravitational perturbations by all planets, but no effects of the thermal forces, were included in this simulation. Major routes of dynamical depletion—mean-motion resonances with Jupiter and the z_1 secular resonance—are shown in light gray. The most notable cases are J9/5, J11/6, and J13/7, all able to destabilize asteroid orbits from tens to hundreds of Myr. A slower depletion track is the resonance J20/11 located at a heliocentric distance of ∼3.49 AU, very near to the current position of (107) Camilla, and J16/9 located at a heliocentric distance of ∼3.54 AU.

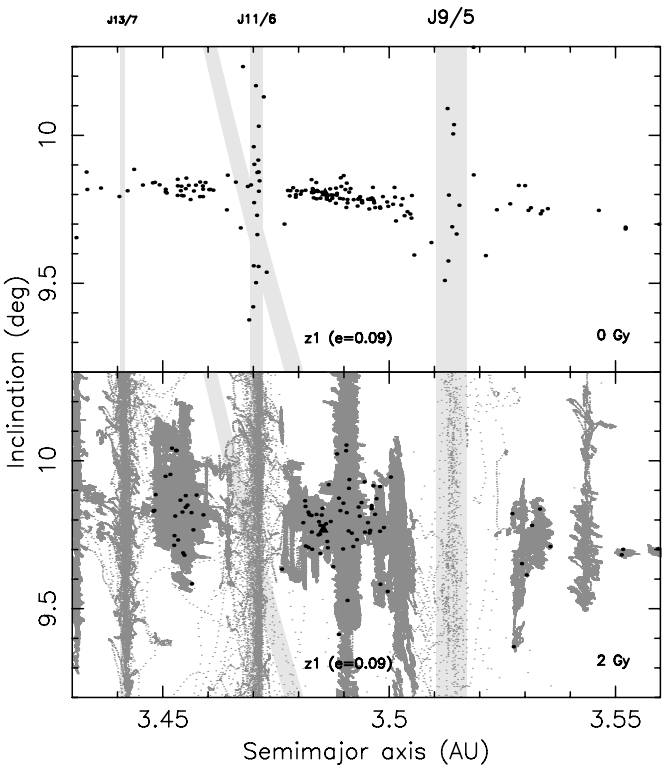

Figure 8. Same as in Figure 7 but now the axes are mean semimajor axis and mean inclination averaged over a 2 Myr running window.

asteroids. This timescale would become about twice as long if we were to take average Yarkovsky drift values for asteroids of their size (recall we used maximum drift rates at zero obliquity). We can thus conclude that a timescale comparable to one billion years is needed to establish the observed unequal eccentricity and inclination distributions at different heliocentric zones of the Sylvia family. We also note that very few asteroids were able to cross the powerful J9/5 resonance: out of 40 objects only one with 5 km size did so and none with the 15 km size (a similar trend toward smaller, and faster drifting objects, having a larger probability to cross the resonance was previously reported for the J9/4 resonance in the Eos family; e.g., Vokrouhlický et al. 2006c). We find it interesting and satisfactory that this estimated minimum age of ∼1 Gyr for the Sylvia family corresponds well with the previously estimated minimum age from dispersal of the fragment initially located below the J11/6 resonance.

Results from our simulation also do not support the idea that some of the smaller asteroids located outward from the J9/5 might have been former Sylvia members that acquired their position by crossing the J9/5 resonance. This is because the fraction of asteroids that would be able to cross this resonance by outward Yarkovsky migration is likely very small. Henceforth, if true members of the Sylvia family reside beyond this resonance they had to be injected onto their orbits during the formation of the family by anomalously large velocities.

3.2. Camilla- and Hermione-zone Analysis

We now address the question of possibly missing families about asteroids (107) Camilla and (121) Hermione. To support our point of view we conducted numerical simulation to see how synthetic families, created about these two asteroids, would dynamically evolve in time. To do so, we first took state vectors of Camilla and Hermione at MJD55000.0 as they result from the available observations. We then created a synthetic population of 200 objects by incrementing the Camilla and Hermione velocities by an isotropic component (we included also Camilla and Hermione as the 201st body). Magnitude of these relative velocities had Maxwellian distribution with a standard deviation of the order of the estimated escape velocity from the respective parent bodies, ∼100 m s^{-1}. To keep things simple, we included gravitational perturbations from all planets but disregarded the effects of the Yarkovsky forces.

With these initial data, we let the system evolve over 2 Gyr and computed average orbital elements of all objects over a 2 Myr wide running window. The first computed mean elements, top panels in Figures 7–10, indicate the structure of the synthetic families immediately after their formation. Because the isotropic velocity field has been used, these are basically elliptic zones with some characteristic dimension following from the assumed dispersal mean velocity. Since (121) Hermione is not far from pericenter at the chosen epoch, the elliptic zone to which the fragments have been launched is slightly tilted in the semimajor axis versus eccentricity projection (Figure 9). We, however, believe that these details cannot change our conclusions.

The orbital stability of different fragments depends on the initial circumstances, most importantly whether they have been injected into, or near to, one of the mean-motion resonances crossing this part of the phase space. The fast evolution in the most powerful of them, J9/5 and J11/6, is actually seen

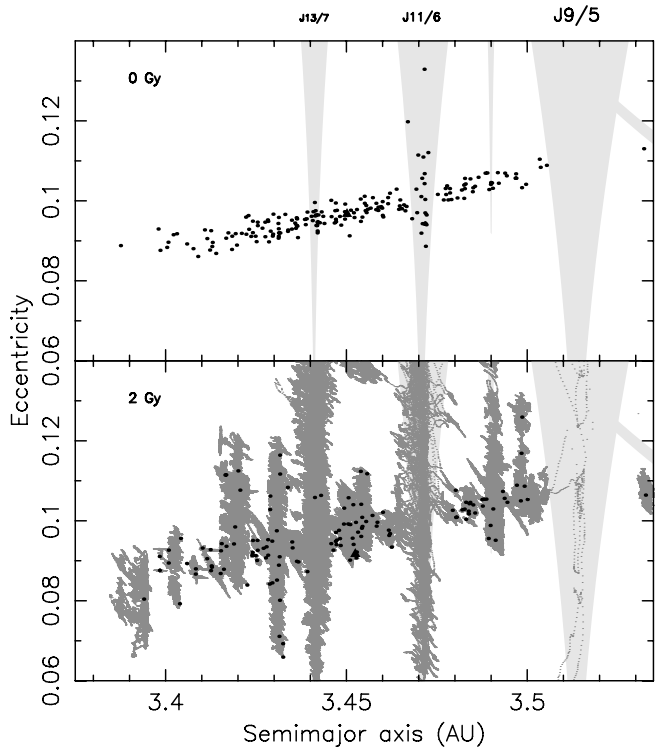

Figure 9. Orbital evolution of a simulated synthetic family about (121) Hermione (black triangle); averaged orbital elements over a 2 Myr running window used on the axes. Top panel shows the first 2 Myr of integration (i.e., the initial simulated family) and bottom panel shows situation after 2 Gyr of evolution. The gray dots are evolutionary tracks of the mean elements and black points are those in the last 2 Myr of the simulation. Gravitational perturbations by all planets, but no effects of the thermal forces, were included in this simulation. Major routes of dynamical depletion—mean-motion resonances with Jupiter and the z_1 secular resonance—are shown in light gray. The most notable cases are J9/5, J11/6, and J13/7, all able to destabilize asteroid orbits from tens to hundreds of Myr. Weaker mean-motion resonances initiated a slow diffusion during our integration timespan of 2 Gyr, but were not yet able to eliminate the asteroids from the family; (121) Hermione itself resides very near to the J24/13 mean-motion resonance with Jupiter.

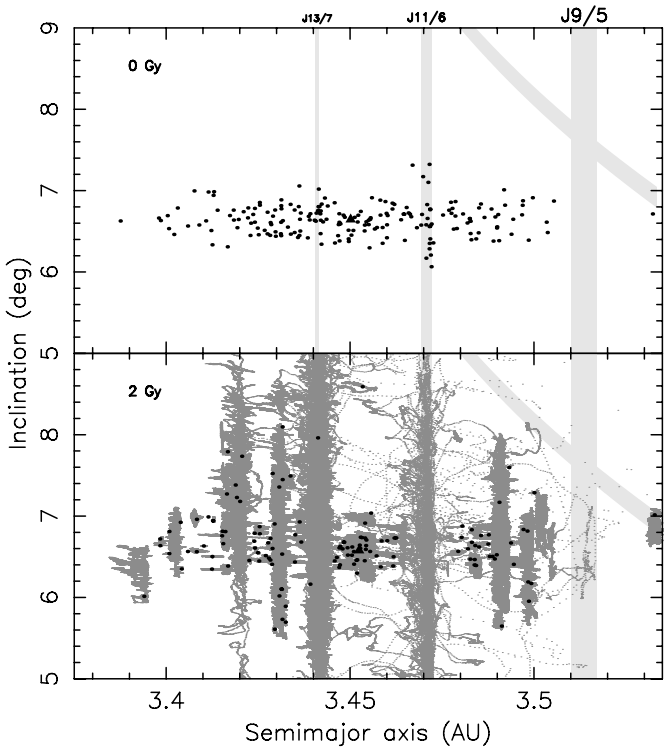

Figure 10. Same as in Figure 9 but now the axes are mean semimajor axis and mean inclination averaged over a 2 Myr running window.

already at the top panels of Figures 7–10. This indicates that the instability timescale in these resonances is shorter than or comparable to the 2 Myr interval used for the element averaging. There is a plethora of weaker mean-motion and secular resonances (out of which the most prominent is z_1 crossing also the zone of the Camilla family) that also result in a long-term instability. Characteristic timescales for such processes may amount to hundreds of Myr up to several Gyr (e.g., Nesvorný et al. 2002) which requires our integration is comparably long. Lower panels in Figures 7–10 show the situation at 2 Gyr. The gray dots are evolutionary tracks of the integrated orbits. We note the instability routes, through which past family members escaped from their initial zone, are marked by discrete, but numerous, weak mean-motion resonances. In the Camilla-family case, the zone crossed by the z_1 resonance exhibits an increased instability level. Overall, from the initial number of 201 simulated members in the two families, 100 escaped from the Camilla vicinity and 65 escaped from the Hermione vicinity. Thus, in the case of Camilla nearly 50% of the initially formed family members dynamically dispersed during the first 2 Gyr of evolution. Only the immediate zone near (107) Camilla showed enough stability to retain family members. There is somewhat more stability in the Hermione case, yet the synthetic family lost about 33% of its initial members in our simulation.

Excessive CPU requirements prevented us to push our simulations to astronomically more relevant ∼4 Gyr timespan. However, based on the available simulation we could argue the putative Camilla and Hermione families would suffer a >40%–70% dynamical erosion if their ages exceeded a couple of Gyr. First, the slow diffusion through weak resonances would continue depleting the families beyond the epoch we reached in our simulation. More importantly though, the thermal (Yarkovsky) forces are capable to move past members of the Sylvia family such that they would reach the weak resonances even if they were not initially located in one of them. The dense enough network of the resonances in this heliocentric zone assures one of the resonances will be on the way. For instance, the characteristic separation of the weak resonances in the Hermione zone is ∼0.01 AU or less. Estimated mean drift rates for 10 km asteroids here is $\sim 10^{-5}$ AU Myr^{-1}, so it takes them roughly 1–2 Gyr to travel between the neighbor resonances. We thus believe that 2–4 Gyr timescale dynamical processes may significantly deplete ancient families about Camilla and Hermione, providing thus a first step toward a solution to understand the existing satellites about these two asteroids and no families around (see Farinella & Vokrouhlický 1999 for a similar argument about depletion of the inner main-belt asteroids).[10]

Yet, it seems unlikely that *all* former members of the two families would have been eliminated by the sole combination of resonant dynamical depletion and Yarkovsky transport in the current planetary configuration. In particular, the immediate zone of (121) Hermione, and to a lesser degree also the core part of the Camilla family, seems rather stable such that we would expect some remaining fragments with slow rate

[10] We note that significant elongation of Camilla and Hermione (e.g., Marchis et al. 2008a; Descamps et al. 2009), as well as Sylvia, helps to assure stability of the satellite orbit over a Gyr timescale (see, e.g., Winter et al. 2009, for the Sylvia system study).

of the Yarkovsky drift to survive even the 4 Gyr timescale. Additionally, faster drifting members may jump over the weak mean-motion resonances; see the one particle in Figure 5 that happened to jump over a rather strong J9/5 resonance. In this way, they would not have been eliminated from the family zone.

4. DISCUSSION AND CONCLUSIONS

The apparent conundrum reached in the last section may only be solved if we assume an additional, perhaps even the most significant, depletion process of the families about Camilla and Hermione. There are two possibilities.

1. Formation of these two families occurred during the last phase of planetary migration that was accompanied by perturbative effects such as the mean-motion resonance sweeping of the Cybele zone.
2. Formation of these two families predates planetary reconfiguration (migration) and their age may be close to the formation of the solar system itself.

In the first possibility, the same processes as involved by Minton & Malhotra (2009) to explain the overall asteroid depletion would be in action to solve the problem (while now thinking on a local scale near the two families). Within the Nice model, the age would thus be constrained to 3.8–3.9 Gyr. Note that this scenario might seem to be in apparent contradiction with the location of these families. For instance, (107) Camilla resides about 0.015 AU above the J11/6 resonance and (121) Hermione resides about 0.01 AU above the J13/7 resonance. This is an order of magnitude less than the estimated shift of these resonances (reflecting the total Jupiter's late drift ∼0.15–0.2 AU; e.g., Tsiganis et al. 2005; Gomes et al. 2005) and one would think that by crossing the orbits of (107) Camilla and (121) Hermione these asteroids would have been eliminated from the Cybele zone. However, as also shown by Minton & Malhotra (2009), the resonance sweeping elimination is incomplete because of the short timescale over which it occurs. Additionally, in the model of Brasser et al. (2009) Jupiter did not acquire its final position by a smooth migration shift but rather a sequence of abrupt jumps due to close encounters with other giant planets or their embryos. In that case, the degree of Cybele zone perturbation may sensitively depend on the chaotic Jupiter's orbit evolution in semimajor axis and excursions of its eccentricity to higher-than-today values.

The second possibility, primordial formation of the Camilla and Hermione families, is an alternative option. Assuming their in situ formation in the Cybele heliocentric zone, one faces the problem of the very survival of (107) Camilla and (121) Hermione in this zone during the dynamical excitation/depletion events associated with planet formation. However, these might be lucky survivors of a much larger primordial population of collisionally formed binary asteroids in the Cybele heliocentric zone and their proximity to the mentioned mean-motion resonances with Jupiter could imply they temporarily resided in them before finally dropping out. An alternative possibility is their implantation from an entirely different source zone, presumably planetesimal disk exterior to giant planets within the process modeled by Levison et al. (2009). Then, however, the C/X-type classification of both (107) Camilla and (121) Hermione warrants consideration that is perhaps part of a more global problem that none of the asteroid families found in the outer parts of the main belt and adjacent resonant populations is not of a spectral D- or P-type (presumably most consistent with objects from the zone exterior to the giant planets; e.g., Mothé-Diniz & Nesvorný 2008, and discussion in this reference).

Exploration viability of these dispersal mechanisms using numerical models is left for further study. Testing the primordial origin, and subsequent elimination, of the families about Camilla and Hermione also should be extended to the cases of other large outer main-belt asteroids with small satellites "missing their families" (recall only (283) Emma possesses a small family of asteroids and (379) Huenna seems to be a member of the Themis family, though not the largest one; Section 1).

Finally, we mention that the age hierarchy of the Sylvia family (1–3.8 Gyr) and putative families about Camilla and Hermione (>3.8 Gyr) established in this work on the basis of long-term orbital evolution finds support in considerations of orbital evolution of the satellite orbits about the respective asteroids. Marchis et al. (2008a, 2008b) argue that the Sylvia satellite system should be rather young, a couple of hundreds of Myr only, while those around Camilla and Hermione could be several Gyr old (these results have been based on considerations of the satellite orbital evolution due to the tidal effects). While depending on the unknown energy dissipation rate in the satellites (see Table 9 in Marchis et al. 2008a), we nevertheless find the consistency of these independent results encouraging.

This research was supported by Czech Grant Agency (grant 205/08/0064) and the Research Program MSM0021620860 of the Czech Ministry of Education.

REFERENCES

Beaugé, C., & Roig, F. 2001, Icarus, 153, 391
Bertotti, B., Farinella, P., & Vokrouhlický, D. 2003, Physics of the Solar System (Dordrecht: Kluwer)
Bottke, W. F., Vokrouhlický, D., Brož, M., Nesvorný, D., & Morbidelli, A. 2001, Science, 294, 1693
Bottke, W. F., Vokrouhlický, D., Rubincam, D. P., & Brož, M. 2002, in Asteroids III, ed. W. F. Bottke et al. (Tucson, AZ: Univ. Arizona Press), 395
Bottke, W. F., Vokrouhlický, D., Rubincam, D. P., & Nesvorný, D. 2006, Annu. Rev. Earth Planet. Sci., 34, 157
Brasser, R., Morbidelli, A., Gomes, R., Tsiganis, K., & Levison, H. F. 2009, A&A, 507, 1053
Brown, M. E., Barkume, K. M., Ragozzine, D., & Schaller, E. L. 2007, Nature, 446, 294
Brož, M. 2006, PhD thesis, Charles Univ.
Brož, M., & Vokrouhlický, D. 2008, MNRAS, 390, 715
Bus, S. J., & Binzel, R. P. 2002, Icarus, 158, 146
Cellino, A., Bus, S. J., Doressoundiram, A., & Lazzaro, D. 2002, in Asteroids III, ed. W. F. Bottke et al. (Tucson, AZ: Univ. Arizona Press), 633
Charnoz, S., Morbidelli, A., Dones, L., & Salmon, J. 2009, Icarus, 199, 413
Descamps, P., et al. 2009, Icarus, 203, 88
Durda, D. D., Bottke, W. F., Enke, B. L., Asphaug, E., Richardson, D. C., & Leinhardt, Z. M. 2004, Icarus, 167, 382
Durda, D. D., Bottke, W. F., Nesvorný, D., Enke, B. L., Merline, W. J., Asphaug, E., & Richardson, D. C. 2007, Icarus, 186, 498
Farinella, P., & Vokrouhlický, D. 1999, Science, 283, 1507
Gil-Hutton, R., & Licandro, J. 2010, Icarus, 206, 729
Gomes, R., Levison, H. F., Tsiganis, K., & Morbidelli, A. 2005, Nature, 435, 466
Ivezić, Z., et al. 2001, AJ, 122, 2749
Karlsson, O., Lagerkvist, C.-I., & Davidsson, B. 2009, Icarus, 199, 106
Knežević, Z., Lemaitre, A., & Milani, A. 2002, in Asteroids III, ed. W. F. Bottke et al. (Tucson, AZ: Univ. Arizona Press), 603
Lagerkvist, C.-I., Moroz, L., Nathues, A., Erikson, A., Lahulla, F., Karlsson, O., & Dahlgren, M. 2005, A&A, 432, 349
Lazzaro, D., Angeli, C. A., Carvano, J. M., Mothé-Diniz, T., Duffard, R., & Florczak, M. 2004, Icarus, 174, 179
Lecar, M., Franklin, F., & Soper, P. 1992, Icarus, 96, 234
Levison, H. F., Bottke, W. F., Gounelle, M., Morbidelli, A., Nesvorný, D., & Tsiganis, K. 2009, Nature, 460, 364
Levison, H. F., & Duncan, M. J. 1994, Icarus, 108, 18

Levison, H. F., Morbidelli, A., Vokrouhlický, D., & Bottke, W. F. 2008, AJ, 136, 1079
Liou, J.-C., & Malhotra, R. 1997, Science, 275, 375
Marchis, F., Descamps, P., Baek, M., Harris, A. W., Kaasalainen, M., Berthier, J., Hestroffer, D., & Vachier, F. 2008a, Icarus, 196, 97
Marchis, F., Descamps, P., Berthier, J., Hestroffer, D., Vachier, F., Baek, M., Harris, A. W., & Nesvorný, D. 2008b, Icarus, 195, 295
Marchis, F., Descamps, P., Hestroffer, D., & Berthier, J. 2005a, Nature, 436, 822
Marchis, F., Hestroffer, D., Descamps, P., Berthier, J., Laver, C., & de Pater, I. 2005b, Icarus, 178, 450
Marchis, F., Kaasalainen, M., Hom, E. F. Y., Berthier, J., Enriquez, J., Hestroffer, D., Le Mignant, D., & de Pater, I. 2006, Icarus, 185, 39
Marzari, F., Scholl, H., Murray, C., & Lagerkvist, C. 2002, in Asteroids III, ed. W. F. Bottke et al. (Tucson, AZ: Univ. Arizona Press), 725
Milani, A. 1993, Celest. Mech. Dyn. Astron., 57, 59
Milani, A., & Farinella, P. 1995, Icarus, 115, 209
Milani, A., & Knežević, Z. 1992, Icarus, 98, 211
Milani, A., & Knežević, Z. 1994, Icarus, 107, 219
Milani, A., Knežević, Z., Novaković, B., & Cellino, A. 2010, Icarus, in press
Milani, A., & Nobili, A.-M. 1985, A&A, 144, 261
Minton, D. A., & Malhotra, R. 2009, Nature, 457, 1109
Mothé-Diniz, T., & Nesvorný, D. 2008, A&A, 492, 593
Nesvorný, D., Beaugé, C., & Dones, L. 2004, AJ, 127, 1768
Nesvorný, D., Bottke, W. F., Vokrouhlický, D., Morbidelli, A., & Jedicke, R. 2006a, in Asteroids, Comets and Meteors, ed. D. Lazzaro et al. (Cambridge: Cambridge Univ. Press), 289
Nesvorný, D., Ferraz-Mello, S., Holman, M., & Morbidelli, A. 2002, in Asteroids III, ed. W. F. Bottke et al. (Tucson, AZ: Univ. Arizona Press), 379
Nesvorný, D., & Vokrouhlický, D. 2006, AJ, 132, 1950
Nesvorný, D., Vokrouhlický, D., & Bottke, W. F. 2006b, Science, 312, 1490
O'Brien, D. P., & Greenberg, R. 2003, Icarus, 164, 334
Parker, A., Ivezić, Ž., Jurić, M., Lupton, R., Sekora, M. D., & Kowalski, A. 2008, Icarus, 198, 138
Pravec, P., & Harris, A. W. 2007, Icarus, 190, 250
Robutel, P., & Laskar, J. 2001, Icarus, 152, 4
Roig, F., Ribeiro, A. O., & Gil-Hutton, R. 2008, A&A, 483, 911
Szabó, Gy. M., Ivezić, Ž., Jurić, M., Lupton, R., & Kiss, L. L. 2004, MNRAS, 348, 987
Szabó, Gy. M., Ivezić, Ž., Jurić, M., & Lupton, R. 2007, MNRAS, 377, 1393
Tsiganis, K., Gomes, R., Morbidelli, A., & Levison, H. F. 2005, Nature, 435, 459
Vokrouhlický, D., Brož, M., Bottke, W. F., Nesvorný, D., & Morbidelli, A. 2006a, Icarus, 182, 118
Vokrouhlický, D., Brož, M., Bottke, W. F., Nesvorný, D., & Morbidelli, A. 2006b, Icarus, 183, 349
Vokrouhlický, D., Brož, M., Farinella, P., & Knežević, Z. 2001, Icarus, 150, 78
Vokrouhlický, D., Brož, M., Morbidelli, A., Bottke, W. F., Nesvorný, D., Lazzaro, D., & Rivkin, A. S. 2006c, Icarus, 182, 92
Warner, B. D., Harris, A. W., Vokrouhlický, D., Nesvorný, D., & Bottke, W. F. 2009, Icarus, 204, 172
Winter, O. C., Boldrin, L. A. G., Vieira Neto, E., Vieira Martins, R., Giuliatti Winter, S. M., Gomes, R. S., Marchis, F., & Descamps, P. 2009, MNRAS, 395, 218
Zappalà, V., Cellino, A., dell'Oro, A., & Paolicchi, P. 2002, in Asteroids III, ed. W. F. Bottke et al. (Tucson, AZ: Univ. Arizona Press), 619
Zappalà, V., Cellino, A., Farinella, P., & Knežević, Z. 1990, AJ, 100, 2030